5666–5678 Nucleic Acids Research, 2012, Vol. 40, No. 12 Published online 8 March 2012
doi:10.1093/nar/gks221

HnRNP L and L-like cooperate in multiple-exon regulation of CD45 alternative splicing

Marco Preußner[1], Silke Schreiner[1], Lee-Hsueh Hung[1], Martina Porstner[2], Hans-Martin Jäck[2], Vladimir Benes[3], Gunnar Rätsch[4] and Albrecht Bindereif[1,*]

[1]Institute of Biochemistry, Justus Liebig University of Giessen, D-35392 Giessen, [2]Divison of Molecular Immunology, Department of Internal Medicine III, Nikolaus-Fiebiger-Center, University of Erlangen-Nürnberg, D-91054 Erlangen, [3]EMBL, Genomics Core Facility, D-69117 Heidelberg and [4]Friedrich Miescher Laboratory, Max Planck Society, Max Planck Institute for Developmental Biology, D-72076 Tübingen, Germany

Received January 20, 2012; Revised February 20, 2012; Accepted February 21, 2012

ABSTRACT

***CD45* encodes a trans-membrane protein-tyrosine phosphatase expressed in diverse cells of the immune system. By combinatorial use of three variable exons 4–6, isoforms are generated that differ in their extracellular domain, thereby modulating phosphatase activity and immune response. Alternative splicing of these *CD45* exons involves two heterogeneous ribonucleoproteins, hnRNP L and its cell-type specific paralog hnRNP L-like (LL). To address the complex combinatorial splicing of exons 4–6, we investigated hnRNP L/LL protein expression in human B-cells in relation to *CD45* splicing patterns, applying RNA-Seq. In addition, mutational and RNA-binding analyses were carried out in HeLa cells. We conclude that hnRNP LL functions as the major *CD45* splicing repressor, with two CA elements in exon 6 as its primary target. In exon 4, one element is targeted by both hnRNP L and LL. In contrast, exon 5 was never repressed on its own and only co-regulated with exons 4 and 6. Stable L/LL interaction requires *CD45* RNA, specifically exons 4 and 6. We propose a novel model of combinatorial alternative splicing: HnRNP L and LL cooperate on the *CD45* pre-mRNA, bridging exons 4 and 6 and looping out exon 5, thereby achieving full repression of the three variable exons.**

INTRODUCTION

Many basic principles of the mammalian splicing machinery are established by now, in particular, how the correct splice sites in the pre-mRNA are recognized (1,2). As we have recently learned from genomewide studies, alternative use of splice sites and its tissue- and developmental control is very common in higher eukaryotes (3,4). Alternative splicing regulation provides not only an important level of gene regulation and enormously increases the coding capacity of our genome, but a global and mechanistic understanding of this process also reveals insight into how mutations can cause human disease (5).

We know only for a few model cases in detail how the spliceosome structure and function is modulated during regulated alternative splicing. A relatively small set of alternative splicing factors, both of the activator and repressor type, interacts with the general splicing machinery, at various stages of splice-site recognition and spliceosome dynamics, and thereby determines the alternative splicing patterns of a very large set of target genes. Target specificity is mediated through *cis*-acting elements of the silencer or enhancer type in the pre-mRNA. Often several splicing regulators cooperate by binding to composite elements consisting of both silencers and enhancers, resulting in a combinatorial network, the so-called splicing code (6).

The *CD45* gene represents one of the first mammalian genes where regulated alternative splicing has been described (7). *CD45* encodes a trans-membrane protein-tyrosine phosphatase expressed in all nucleated hematopoietic cells, studied in particular in T-lymphocytes. As a result of the combinatorial use of three variable exons 4–6, five different isoforms are generated (8–10), and the extracellular glycosylated domain is expressed to different extents. Thereby, the CD45 dimerization potential and phosphatase activity are regulated, modulating the threshold of T-cell activation and the immune response (11). Specifically, resting T-cells switch from the predominant 'full-inclusion' form, R456, carrying all three variable

*To whom correspondence should be addressed. Tel: +49 641 9935 420; Fax: +49 641 9935 419; Email: albrecht.bindereif@chemie.bio.uni-giessen.de

The authors wish it to be known that, in their opinion, the first three authors should be regarded as joint First Authors.

exons, and a mix of 'partial-inclusion' forms (R45, R56 and R5), to the R0 form, in which all three exons 4–6 are skipped.

For B-cells, the functional role of CD45 is less well studied, nevertheless, it is known that *CD45* alternative exon skipping similarly contributes to the cessation of the primary immune response (12). Upon activation, B-cells switch to the expression of shorter CD45 isoforms (13,14), consistent with the expression of the R0 form in terminally differentiated plasma cells.

What *cis*-acting elements and which factors regulate the use of individual variable exons 4–6 has been studied in detail by Lynch and coworkers, using a human T-cell line, JSL1, which can be activated *in vitro* (15). In combination with mutational analyses of minigenes carrying single variable exons, several activation-responsive sequence (ARS) elements, splicing silencers and enhancers were mapped, and hnRNP L (called L in the following) was characterized as a repressor, binding to CA-rich silencer elements in exons 4–6 (16,17). In addition, based on independent screening approaches (18–20), hnRNP L-like (called LL in the following) was identified as an activation-induced repressor of *CD45* alternative splicing, which *in vitro* binds to the exon 4 ARS element, but not to exon 5 (18,21). However, how the L/LL proteins cooperate to determine combinatorial alternative splicing of *CD45* has not been analyzed. Very recent work has added another layer to the complex *CD45* splicing regulation, co-transcriptional recruitment of CTCF to exon 5 genomic DNA, resulting in RNA polymerase II pausing and increased exon 5 inclusion (22).

L is a multifunctional RNA-binding protein with roles in RNA stability, IRES-mediated translation, intron-less mRNA export [see (23) for references], riboswitch activity in the *VEGFA* mRNA (24), differential polyadenylation and alternative splicing, including L autoregulation (16,23,25). In contrast, the paralog LL, which shares with L 68% amino acid sequence homology and the same domain organization of four RNA-recognition motifs (RRMs; see 25), appears to be specialized to splicing-regulatory roles in lymphocytes (18–20; this study). Based on these studies there is clearly a consensus on hnRNP LL acting as a major repressor of the *CD45* variable exons, and genomewide analyses reported additional hnRNP LL targets. However, since extensive validation and further biochemical analyses of these targets have not been performed yet, a role of hnRNP LL as a master regulator of immune-relevant genes in T-cells (19) remains to be confirmed.

We had initially established the RNA-binding specificity of L by *in vitro* SELEX (26), which revealed as high-affinity binding sites CA-repeat sequences, but also certain CA-rich motifs (CACA and ACAC as high-score, and TACA and CACC as low-score motifs). In natural binding sites often closely spaced clusters of such short motifs occur, most likely reflecting multiple RNA interactions of a single L molecule, mediated through its four RRMs (for examples, see 23,26). The RNA-binding specificity of LL is similar to that of L, but distinct (18,23), and the molecular basis for this is still unknown.

Regarding alternative splicing regulation by L versus LL, we had identified several L targets, based on a genomewide CA-motif search combined with alternative splicing evidence (26). More recently, we used a combined strategy of splice-sensitive microarray analysis and RNAi knockdown (25) to identify more alternative splicing targets of L; surprisingly, no LL targets were found in HeLa cells. We noted in the same study that in HeLa cells, L is ~10-fold more abundant than LL. In sum, these studies confirmed the global role of L as an alternative splicing regulator, and are consistent with the LL paralog acting in a cell-type-specific manner.

Here, we focus on alternative splicing of the three variable exons in *CD45*, using it as a paradigm for the complex type of combinatorial exons. In comparison to other modes of alternative splicing (single-exon skipping; alternative 5′ and 3′ splice sites), we do not yet understand well what determines the variable use and combinations of several adjacent alternatively spliced exons. Both paralogous L/LL proteins target the three-exon unit in *CD45*, and we address the general question of how two RNA-binding proteins cooperate in generating a complex alternative splicing pattern. We establish here and mutationally analyze a new *CD45* minigene system that contains all three regulated exons 4–6. In addition, we identify and make use of B-cell lines, whose LL expression dramatically differs, to characterize the L/LL-mediated splicing regulation of *CD45*.

In sum, we conclude: First, the three-exon unit can be skipped only in the presence of LL. Second, exons 4 and 6 provide the major targets of L and LL, with LL preferentially binding to two silencer elements in exon 6, but also to a silencer element in exon 4; in contrast, exon 5 can only be corepressed in combination with exons 4 and 6. Third, L and LL interact with each other, depending on *CD45* RNA and variable exons 4 and 6, but not on exon 5. Taken together, our data strongly argue for a model, whereby exons 4 and 6 are repressed by L and LL interacting with each other on the *CD45* RNA, and exon 5 is corepressed by looping out, resulting in full skipping of the three-exon unit.

MATERIALS AND METHODS

Human B-cell lines and RNA-Seq analysis

Human B-cell lines Nalm-6 (DSMZ ACC128), Ramos (DSMZ ACC603), BJAB (ATCC HB-136), ARH-77 (DSMZ ACC512), HS-Sultan (ATCC CRL1484), Raji DSMZ ACC319), IM-9 (DMSZ ACC117), Amo-1 (DSMZ ACC538), NCI-H929 (DSMZ ACC 163), JK6L (27), OPM-2 (DSMZ ACC50), RPMI-8226 (DSMZ ACC402), U-266 (DSMZ ACC9), XG-1 (28) and DG75 (DSMZ ACC83) were grown in RPMI medium (Invitrogen), or LP-1 (DSMZ ACC41) cells in IMDM medium (Invitrogen). Both media were supplemented with 10% FBS, 2 mM L-glutamine, 1 mM sodium pyruvate, 100 U/ml penicillin/streptomycin and 50 μM β-mercaptoethanol. The growth medium for XG-1 additionally contained 2 ng/ml IL-6. For western-blot analysis cells were harvested and lysed with RIPA buffer

(50 mM Tris pH 8.0, 150 mM NaCl, 1% NP40, 0.5% deoxycholate, 0.1% SDS). For LL overexpression, 2×10^6 DG75 cells were transfected with 0.05, 0.2, 0.5, or 2 μg LL-V5-His plasmid (for RNA-Seq, 2 μg) or, as a control, 1 μg eGFP (also for RNA-Seq), using the Nucleofector™ kit V (Amaxa™) and program T15. After 24 h cells were harvested, and RNA was isolated, using Trizol (Invitrogen) and the RNeasy kit (Qiagen), followed by RQ1 DNase digestion. Total RNA was analyzed by RT-PCR or Solexa RNA-Seq; for details on the data analysis, see Rösel *et al*. (29). RNA-Seq sequence read data have been uploaded to the GEO database at NCBI (GSE 33013).

Constructs and DNA oligonucleotides

Expression constructs. To generate hnRNP L- and hnRNP LL expression constructs with N-terminal FLAG tags (FLAG-L; FLAG-LL), hnRNP L full-length cDNA was released from the plasmid pFASTBAC HTb-hnRNP L (30) by cutting with HindIII and XhoI. For FLAG-LL, the hnRNP LL reading frame was cut out by EcoRI and SalI from the pGEX-hnRNP LL construct (25). Vector pcDNA3.1 was digested with HindIII and XhoI, and the FLAG-tag fragment was generated by annealing oligonucleotides with HindIII and EcoRI ends, followed by triple ligation.

For the hnRNP LL expression construct with a C-terminal V5-His tag, the hnRNP LL open reading frame was cloned into TOPO vector pcDNA3.1/V5-His-TOPO (Invitrogen), resulting in pcDNA3.1/hnRNP LL-V5-His.

CD45 wild-type. To generate the CD45 wild-type (CD45 WT) minigene, an intermediate, containing three different parts was cloned into pcDNA3.1, using HindIII and ApaI: first, 23 bp of exon 2 joined with exon 3, together with 130 bp of downstream intron 3 sequence; second, the variable exon 4 and flanking intronic sequences (upstream 80 bp and downstream 20 bp); third, the constitutive exon 7 with 130 bp of upstream intron 6, and 20 bp of downstream intron 7. For further cloning steps an XhoI site was inserted in intron 3, 80-bp upstream of the exon 4 3′ splice site, and an EcoRI site in intron 4, 20-bp downstream of the exon 4 5′ splice site. Subsequently exon 4 was replaced by an insert containing all three variable exons and shortened intervening introns (for each exon: 80-bp upstream and 20-bp downstream sequence), produced by three-step PCR, using the previously inserted XhoI and EcoRI sites.

Single-exon replacement by heterologous sequences. Inserts replacing the exonic sequence of exons 4, 5 or 6 by DUP exon 2 sequence (31) of the same length were generated by PCR, without altering the splice sites (first and last 3 nt of each exon were left unchanged). For each construct, individual restriction sites were used for cloning into the CD45 WT construct: for the DUP-ex4 insert, XhoI and EcoRI; for the DUP-ex5 mutant, XhoI and a PPuMI site in intron 5; for the DUP-ex6 mutant, PpuMI and EcoRI.

Mutational analysis of potential silencer elements in exons 4 and 6. All mutants were constructed using site-directed mutagenesis PCR. The mutant in the silencer element of exon 4 (4/5′CA) was cloned into the CD45 WT construct using XhoI and EcoRI. Initially, exon 6 mutants were created by PCR, using CD45 WT as a template (6/5′CA, 6/mCA, 6/3′CA). The double mutation in exon 6 (6/m + 3′CA) was introduced by two-step PCR, using the single mutants (6/mCA, 6/3′CA) as template. For the combined mutant of exons 4 and 6 (4/5′CA + 6/m + 3′CA) the insert, containing the exon 6 mutations, was cut out from 6/m + 3′CA and inserted into the 4/5′CA construct, using PpuMI and EcoRI.

For sequences of DNA oligonucleotides, see Supplementary Data.

CD45 mutational analysis and knockdown/overexpression of L/LL proteins in HeLa cells; RT-PCR assays of alternative splicing

siRNA-mediated knockdown in HeLa cells was performed as previously described (25). Three days after siRNA transfection, 6 μg of CD45 WT plasmid was transfected, using FuGENE HD transfection reagent (Roche), according to the manufacturer's protocol. After 24 h, RNA was isolated, as described earlier. Total RNA (1 μg) was reverse transcribed by the qScript™ Flex cDNA kit (Quanta), using the minigene-specific primer BGHrev. PCR was performed with different *CD45*-specific primer combinations. The knockdown efficiency was determined by western blotting.

For transfections of *CD45* minigenes, HeLa cells were seeded onto 6-well plates (1.5×10^5 cells per well), 1 day before transfection. Transfections were performed with *CD45* minigene variants (4 μg), using TurboFect *in vitro* transfection reagent (Fermentas), according to the manufacturer's instructions. After 24 h, RNA was isolated, as described earlier. Total RNA (0.5 μg) was reverse-transcribed by the qScript™ cDNA synthesis kit (Quanta). All PCR-products obtained for *CD45* primers to exons 3 and 7 were further confirmed by TOPO-cloning (Invitrogen) and Sequencing (SeqLab).

For (co-)transfections of L, LL and *CD45* minigenes, HeLa cells were seeded onto 6-cm culture dishes (5×10^5 cells per dish), 1 day before transfection. Co-transfections, using FLAG-L (1 μg), FLAG-LL (2 μg), or eGFP vector (1 μg), with *CD45* minigene variants (4 μg), were performed, using TurboFect *in vitro* transfection reagent (Fermentas), according to the manufacturer's instructions. After 24 h, RNA was isolated and analyzed as described earlier.

In vitro RNA-binding of hnRNP L proteins: biotin-RNA pulldown assays

Template DNAs for *in vitro* transcription (AmpliScribe™ T7-Flash™ transcription kit, Epicentre Biotechnologies) of *CD45* exons 4, 4/5′CA, 5, 6, 6/5′CA, 6/mCA, 6/3′CA, 6/m + 3′CA, 6/DUP, 4-5-6 and 4*-5-6* were PCR-amplified from the respective *CD45* constructs, thereby introducing the T7 promotor (Figure 5A and B, lanes 1–14). Due to PCR problems, the DUP-substituted

RNAs (DUP-ex4, -ex5 and -ex6; Figure 5B, lanes 15–18) were generated from EcoRI-linearized constructs. The resulting transcripts additionally contain upstream exons 2 and 3, a shortened intron 3 and downstream the first 20 nt of intron 6.

Purified RNAs were chemically 3′-biotinylated (32), and 40 pmol of each were bound to 20 µl of blocked NeutrAvidin agarose beads (Thermo Scientific), by incubation overnight at 4°C in a total volume of 200 µl WB300 (20 mM HEPES pH 7.5, 1 mM DTT, 10 mM $MgCl_2$, 300 mM KCl, 0.01% NP-40). Bound biotinylated RNAs were then incubated for 30 min at room temperature with 30 µl of HeLa nuclear extract (CILBIOTECH, Mons, Belgium) in a final volume of 100 µl WB100 (as WB300, with 100 mM KCl). After precipitation and three wash steps (100–300 mM KCl, as indicated), bound protein was released with 2× SDS loading buffer and incubation at 95°C for 5 min, followed by western-blot analysis.

L-LL interaction in HeLa and DG75 B-cells: FLAG pulldown and western blot

LL overexpression in HeLa cells for FLAG immunoprecipitation was adjusted to 10-cm culture dishes [FLAG-LL (3.3 µg) with or without *CD45* minigene variants (each 6 µg)]. After 24 h, cells were harvested and lysed with RIPA buffer (see above). In a control lysate, RNA was digested with RNase A (final concentration 0.2 mg/ml) at room temperature for 20 min. The lysates were incubated with 20 µl packed anti-FLAG M2 affinity gel (Sigma) overnight at 4°C. Beads were washed four times with 1 ml TBS-T (50 mM Tris pH 8.0, 150 mM NaCl, 0.05% Tween), proteins were eluted with 2× SDS-loading buffer and analyzed by western blotting.

For western-blot analysis, cells were resuspended (or lysed in RIPA buffer, as described) in 2× SDS loading buffer, separated on a 10% SDS polyacrylamide gel and transferred to a Hybond ECL nitrocellulose membrane (GE Healthcare). Anti-L (4D11, Sigma), affinity-purified anti-LL (25), anti-FLAG (Sigma), anti-γ-tubulin (GT88; Sigma) and anti-GAPDH (Sigma) were used as primary antibodies, HRP-conjugated anti-mouse or anti-rabbit IgG (Sigma) as secondary antibodies. The blots were developed using the lumi-light western-blotting substrate (Roche).

For FLAG immunoprecipitation from DG75 B-cells, cells were transiently transfected with 0.5 µg of FLAG-LL, or, as a control 0.5 µg eGFP (Amaxa^{TM}), as previously described. After 24 h, cells were harvested and lysed with TBS buffer, containing 1% Triton X. Immunoprecipitation was performed as described for HeLa cell lysates, followed by western-blot analysis, using anti-hnRNP L; -hnRNP LL, and, as a control, anti-GAPDH antibodies (see above).

RESULTS

Differential hnRNP LL expression in human B-cell lines: hnRNP LL as major repressor of CD45 exons 4–6

To address the role of the splicing repressor hnRNP LL in *CD45* alternative splicing during B-cell development, we analyzed LL protein levels in several human B-cell lines (Figure 1A). Western-blot analysis showed high expression of LL in all myeloma cell lines, which represent terminally differentiated plasma cells (right panel). In contrast, in most cell lines derived from earlier stages, LL expression was low or undetectable (left panel). The pre B-cell line Nalm-6 and lymphoblastoid cell lines ARH-77 and IM-9 that are activated and EBV-transformed, displayed no or only very low expression of LL. The mixed pattern of LL expression in Burkitt lymphoma B-cell lines Ramos, BJAB, HS-Sultan and Raji might be a result of their heterogeneous activation and transformation status. Unlike LL, hnRNP L expression was not developmentally regulated, and most cell lines tested expressed similar levels.

Next we compared the *CD45* splicing pattern of two cell lines that express similar levels of L, but differ in LL expression: the Burkitt lymphoma B-cell line DG75, which does not express detectable levels of LL, and the myeloma cell line U-266 with high levels of LL (Figure 1B). Consistent with LL's role as a splicing repressor, in DG75 cells the variable exons were mainly included (R56 and R456 forms), while U-266 cells predominantly produced the R0 form, reflecting skipping of exons 4–6. In addition, overexpression of LL in DG75 cells was sufficient to switch *CD45* splicing to the R0 form in a dose-dependent manner (Figure 1C).

To further analyze the complex combinatorial splicing pattern of the three variable *CD45* exons, we used RNA-Seq data, based on a total of 53.5 million Illumina-Solexa 76-bp single-end reads (24.5 million for GFP control, 29 million for LL overexpression). Figure 2 summarizes the results, comparing DG75 cells after GFP-control transfection (in blue) versus LL overexpression (in red; for western-blot analysis, compare Figure 1C, lanes 1 and 5). For the *CD45* genomic region between exons 3 and 7, the read densities (top), the ratio of read densities after LL and GFP overexpression, as well as junction read counts (bottom) are given. As expected, the read densities of exons 4–6 were reduced after LL overexpression. However, comparing the various exon junctions was more informative: Most striking were the junction read counts that represent complete skipping of exons 4–6 (R0 form): One over 41 reads indicates that this form changed most dramatically after LL overexpression. Similarly, skipping of exon 6 (i.e. exons 5 and 7 junction reads) increased from one to nine counts, indicating LL's role as major exon 6 repressor; less dramatic, but significant, was the repressor effect of LL for other exon junctions.

CD45 exon-specific repression by L and LL

To analyze in detail the combinatorial regulation of the three variable exons, we constructed a *CD45* minigene carrying exons 4–6 in between the flanking constitutive exons 3 and 7, with the intron sequences shortened to ~100 nt (Figure 3, schematic below panel B). *CD45* minigenes were transfected in HeLa cells, which contain both L/LL proteins, allowing knockdown studies of either

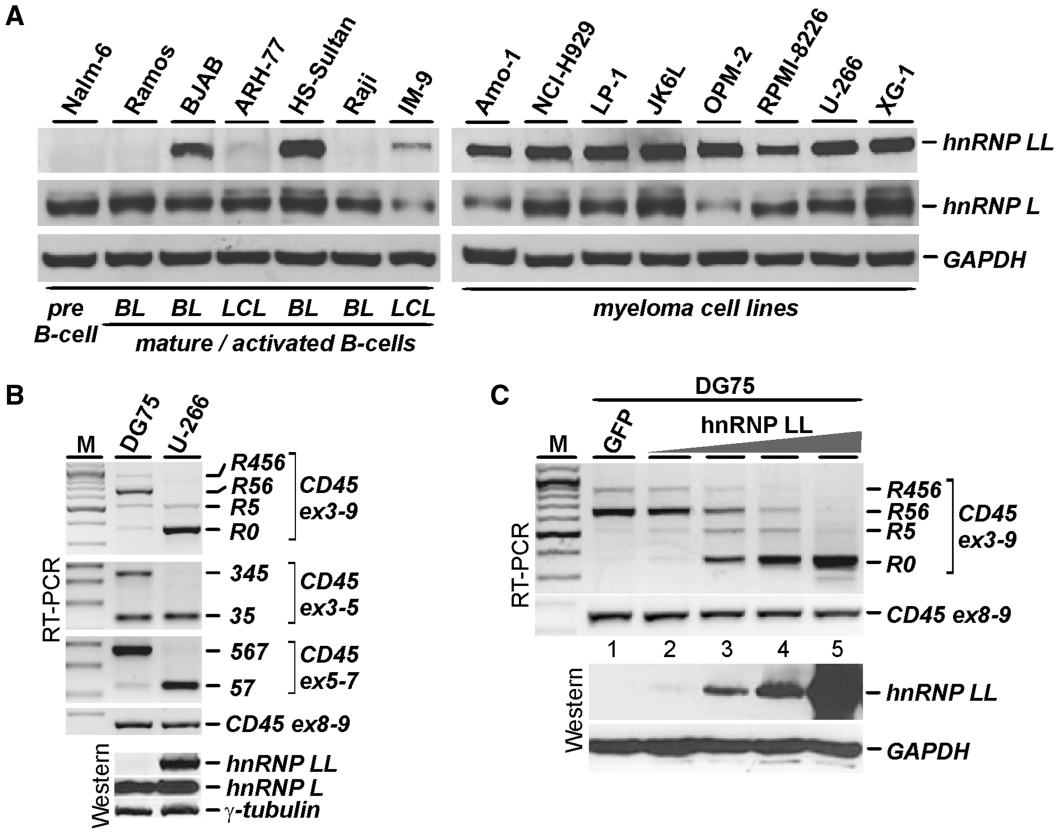

Figure 1. HnRNP LL is differentially expressed in B-cell lines and regulates *CD45* alternative splicing. (**A**) High LL expression correlates with the plasma cell stage of B-cell development, while L is expressed at similar levels in most of the B-cell lines tested (names of cell lines above the lanes). Lysates from B-cell lines derived from early, mature or activated stages of B-cell development [left panel: pre B-cell stage (pre), lymphoblastoid cell lines (LCL) and Burkitt lymphoma B-cell lines (BL), as indicated below] and from plasma cell-derived B-cell lines (right panel: myeloma cell lines) were analyzed by western blot for L/LL (GAPDH as a loading control). (**B**) *CD45* alternative exon repression correlates with LL expression levels. *CD45* alternative splicing analysis by RT-PCR, comparing two different B-cell lines (Burkitt lymphoma line DG75, myeloma cell line U-266). Primer pairs (*CD45* ex3–9, 3–5 and 5–7) and products (*CD45* splice forms R456, R56, R5, R0; exons 4 and 6 inclusion/skipping forms; constitutive ex8–9 product) are labeled on the side. *M*, DNA size markers. Below, the expression of LL, L and γ-tubulin were detected by western blotting. (**C**) HnRNP LL overexpression is sufficient for *CD45* exons 4–6 skipping and the generation of the R0 form. DG75 cells were transfected with increasing amounts of LL-V5-His plasmid (0.05, 0.2, 0.5 or 2 μg), or as a control, GFP (1 μg). Total RNA was analyzed by RT-PCR (top) for *CD45* alternative splicing [products and primer pairs indicated on the right, as in panel (B)]. *M*, DNA size markers. Below, LL overexpression was assessed by western blotting, with GAPDH as a control.

protein, and which do not express endogenous *CD45*, allowing mutational analysis.

First, L and LL were individually and in combination downregulated by RNAi (see Figure 3A for western-blot analysis). Second, the *CD45* minigene was transfected, followed by RT-PCR analysis, using these primer combinations (Figure 3B): exons 3–7, to detect all possible variable-exon combinations; exons 5–7, 3–5 and 4–6, for detection of specific use of exons 6, 4 and 5, respectively. In the control knockdown, we detected four major RT-PCR products, reflecting the R456, R45, R5 and R0 forms (lane 2). L downregulation led to a significant shift towards the inclusion products, R45 and R456 (lane 3). However, after downregulation of LL and of both L/LL, the full-inclusion form R456 was almost exclusively formed (lanes 4 and 5). The low level of remaining R0 form may be due to the minigene context and its shortened introns, which brings the flanking exons into closer proximity. In sum, we conclude that LL acts as a much stronger repressor of all three variable *CD45* exons than L.

We also analyzed each of the three variable exons separately (lanes 6–17). Thereby we detected only a subset of splice forms carrying the two respective flanking exons. Exon 6 did not respond significantly to L knockdown, but the LL and the double knockdown resulted in almost complete exon 6 inclusion (lanes 6–9). In contrast, exon 4 inclusion weakly increased upon L, and strongly upon LL and double knockdowns (lanes 10–13). Finally, exon 5 was never individually repressed (lanes 14–17). We conclude that both hnRNP L proteins act as repressors, but their functional contributions clearly differ: L acts only on exon 4; LL strongly represses both exons 4 and 6.

Mutational analysis of CD45 exons 4 and 6: cooperation between multiple silencer elements

We next used our *CD45* minigene to study the role of putative L/LL binding sites of exons 4 and 6, the major targets of regulation, in determining the complex

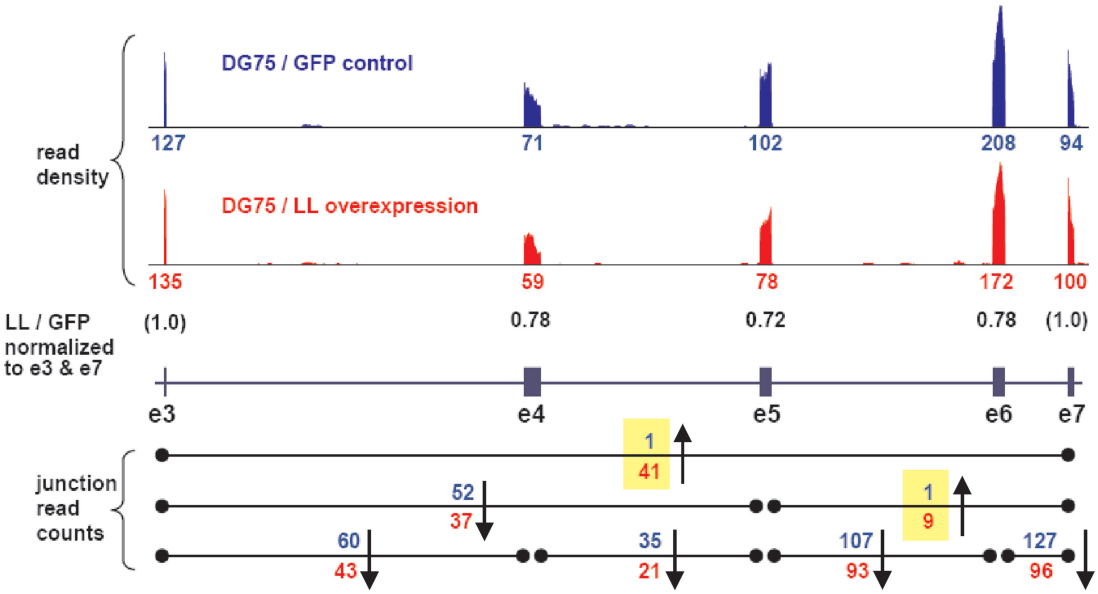

Figure 2. RNA-Seq analysis of *CD45* alternative splicing in DG75 B-cells. LL (or as a control, GFP) was overexpressed in DG75 B-cells, followed by RNA-Seq analysis of total RNA. On the top, the read densities across the *CD45* exons 3–7 region are represented, comparing GFP control (in blue) and LL overexpression (in red). The numbers below indicate the respective read densities of exons 3–7. In the middle, the ratios of LL/GFP exon read densities, normalized to the constitutive exons 3 and 7, are given, below, the exon–intron structure. The bottom part summarizes the absolute junction read counts, with the arrows indicating changes in a particular splice event after LL overexpression (↑ increase; ↓ decrease).

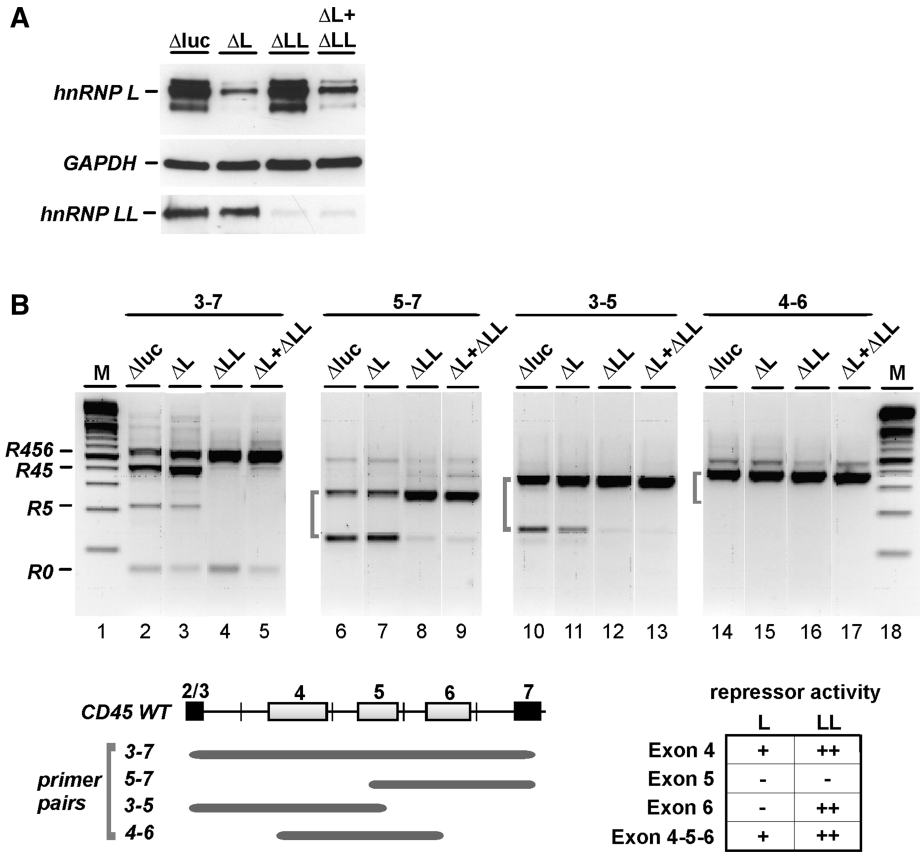

Figure 3. *CD45* alternative splicing of a minigene in HeLa cells: specific repression of *CD45* alternative exons 4–6 by hnRNP L and LL. (**A**) L (ΔL), LL (ΔLL), or both of them (ΔL + ΔLL) were RNAi-downregulated in HeLa cells, including a control luciferase knockdown (Δluc), as confirmed by western blot for L, LL and GAPDH. (**B**) Following knockdown, the CD45 WT minigene was transfected, and *CD45* alternative splicing was assayed by RT-PCR (primer pairs indicated above the lanes, and schematically shown below). The RT-PCR products indicative of the R456, R45, R5 and R0 forms (for primer pair 3–7), or for the inclusion/skipping-products (for primer pairs 5–7, 3–5 and 4–6; see brackets) are marked on the left. All lanes come from a single gel, but were rearranged for clarity. *M*, DNA size markers. Below, the repressor activities of L versus LL for *CD45* exons 4–6, as well as for the entire exons 4–6 unit are summarized (++ strong; + weak; – not significant).

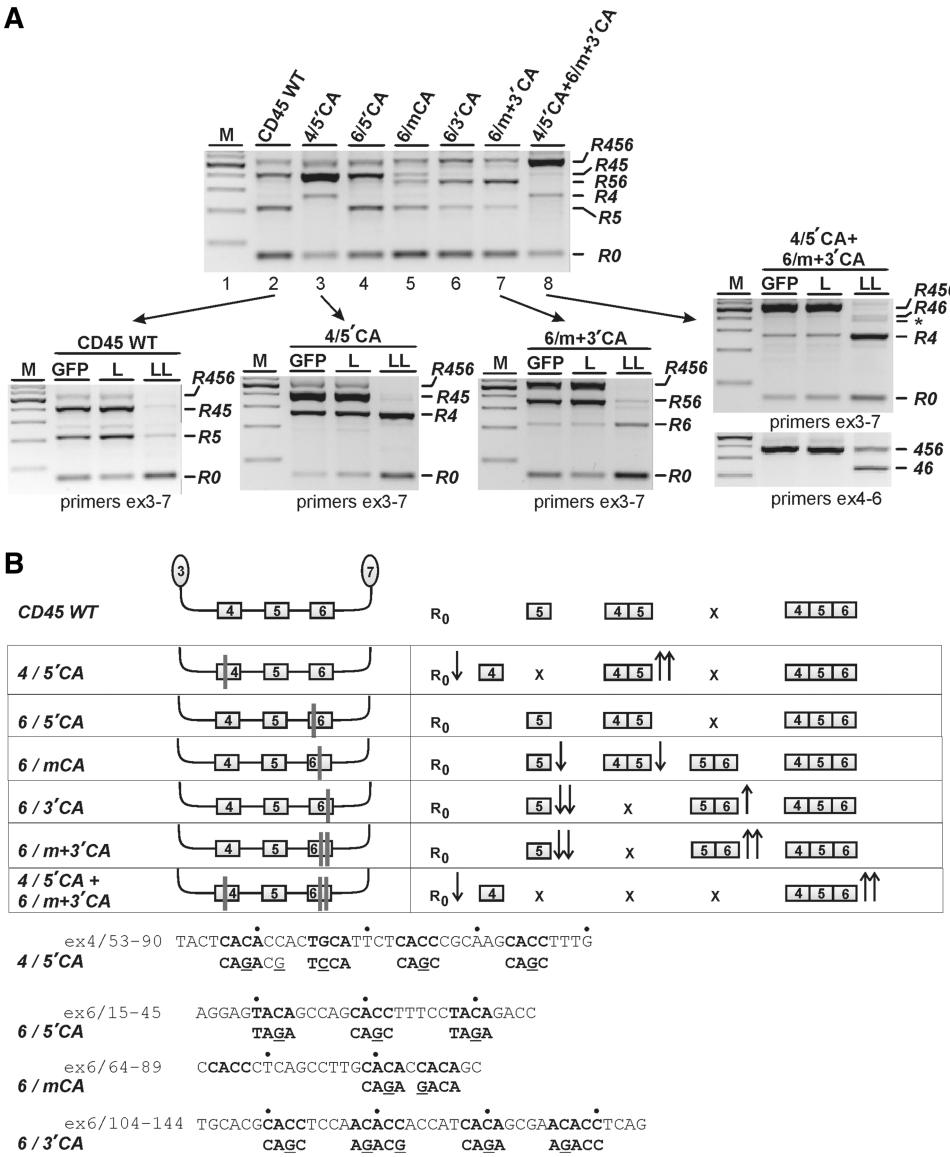

Figure 4. Mutational analysis of *CD45* silencer elements in exons 4 and 6. (**A**) CD45 WT minigenes and mutant derivatives [as indicated above the lanes; see panel (B) for schematic representations] were transfected in HeLa cells, followed by RT-PCR with primers against *CD45* exons 3 and 7 (products represented on the right). For CD45 WT and mutants 4/5′CA, 6/m + 3′CA and 4/5′CA + 6/m + 3′CA, additional cotransfections were done with GFP (as control), with FLAG-L or FLAG-LL (as indicated above the lanes), followed by RT-PCR assays with exons 3–7 or 4–6 primer pairs (as indicated). The asterisk marks an unspecific PCR product, which could not be identified. *M*, DNA size markers. (**B**) Summary of *CD45* mutant minigenes used (the position of mutations marked by thick vertical lines). The mutated nucleotide positions in exons 4 and 6 are specified below, in each case with the CA elements in bold letters and the mutations underlined. Spliced *CD45* isoforms are represented on the right side, with single and double arrows indicating changes compared to wild-type.

alternative splicing pattern (Figure 4; see panel B for a schematic of minigenes, mutations introduced and splicing phenotypes).

As seen earlier, splicing of CD45 WT resulted in a mixture of R456, R45, R5 and R0 forms (lane 2). Mutation of the single CA cluster of L/LL binding sites in exon 4 (4/5′CA) resulted in several striking changes: The R45 form strongly increased; the R5 form disappeared, and instead, a new splice form with only exon 4 included appeared (R4); in addition, the R0 form decreased (lanes 2 and 3). The new R4 from indicates that the 5′CA mutation in exon 4 inactivated a silencer element. The concomitant strong increase in the R45 form argues for efficient corepression of exons 4 and 5. Moreover, LL overexpression with the 4/5′CA mutant minigene completely shifted the splicing pattern to the R4 and R0 forms, different from CD45 WT, where only the R0 form was observed (compare insets below lanes 2 and 3). In contrast, overexpression of L had no effect, probably due to the high levels of endogenous L.

Next, a series of three exon 6 mutations were assayed, designed to selectively inactivate the 5′ terminal, the middle and the 3′ terminal CA cluster. Compared with alternative splicing of CD45 WT, the 6/5′CA mutation

did not result in any significant changes, indicating that the 5′CA cluster does not play an important role in exon 6 repression (lane 4).

Mutating the middle CA element in exon 6 (6/mCA; lane 5), however, did change the splicing pattern: Both the R45 and R5 forms decreased, and a new combination of exons 5 and 6 appeared, the R56 form. This suggests that the mCA mutation inactivated a silencer element in exon 6, resulting in more exon 6 inclusion, which appears to be coupled with exon 5, explaining the new R56 form.

Inactivating the 3′ terminal CA cluster in exon 6 (6/3′CA; lane 6) further enhanced all effects observed for the mutated middle element: increased R56 form, decreased R5 form and undetectable R45 form. This indicates that the 3′ terminal CA cluster functions as a more potent silencer than the middle CA cluster does.

Combining the mutations of both middle and 3′ terminal silencers in exon 6 (6/m + 3′CA; lane 7 and insert below) further enhanced the effects seen with both separate mutations. This strongly argues for two functionally independent silencers. Interestingly, after LL overexpression, exon 6 by itself could be detected (R6 form), further supporting the silencer role of both CA clusters.

The combination of mutations in exons 4 and 6 described earlier (4/5′CA + 6/m + 3′CA; lane 8 and insert below) showed the most dramatic splicing phenotype: The full-inclusion form R456 was strongly increased, reflecting the combined inactivation of all three silencers in exons 4 and 6; in addition, we detected no partial-inclusion forms anymore (R56 and R5). Instead, the R4 form appeared, and this unusual form strongly increased upon LL overexpression, consistent with what we previously found for the 4/5′CA mutant (compare lanes 8 and 3, and inserts below). Under these conditions, another unusual, minor spliced form was detected, R46, with exons 4 and 6 included, but not exon 5; only in this case, when silencers in both exons 4 and 6 were mutated, we have seen this exceptional joining of exons 4 and 6.

Stable complex formation of L and LL on CD45 exons 4 and 6: mutational analysis *in vitro*

In order to correlate these splicing changes of *CD45* mutant minigenes with L/LL binding, we next assayed the *in vitro* interaction with WT and mutant single-exon 4–6 RNAs (Figure 5A). RNAs were 3′-biotinylated and bound to Neutravidin agarose, followed by incubation in HeLa nuclear extract and western-blot analysis of bound protein. Binding efficiencies were generally lower for L than for LL, which may be due to their different protein levels in nuclear extract. Comparing the binding activities of L versus LL, both proteins behaved similarly: Exons 4 and 6 were efficiently bound, whereas exon 5 as well as the mutant exon 4 with the inactivated silencer element (exon 4/5′CA) did not significantly bind L/LL (lanes 1–5). L/LL association greatly differed for the four exon 6 mutant RNAs (lanes 6–10): Whereas mutation of the 5′ terminal CA element had only a minor effect (exon 6/5′CA), mutations of both middle (/mCA) and 3′ elements (/3′CA) greatly reduced L/LL binding, and their combination (/m + 3′CA) abolished L/LL binding, similarly as substitution of the entire exon 6 (/DUP).

In sum, these *in vitro* binding data demonstrate that both L and LL bind to exons 4 and 6; in contrast, binding to exon 5 is insignificant. Mutations in the three silencer elements of exon 6 differentially affected L/LL interaction, correlating well with their effects on alternative splicing (see Discussion).

Next we tested, whether the combination of all three variable exons in *cis* influences the affinities for L/LL. Biotinylated RNAs, containing exons 4–6 together with shortened intervening introns, were analyzed for L/LL binding under different stringencies of washing (Figure 5B). The LL binding efficiency for the exons 4-5-6 RNA (lane 4) reflected combined binding to the individual exons (panel A, lane 2, and panel B, lanes 2 and 3). Increasing stringency during washing to 300 mM KCl reduced LL affinity for both exon 6 and for exons 4-5-6 by ~50% (panel B, compare lanes 3 and 4 and 12 and 13).

In contrast to LL, binding of L to exons 4-5-6 RNA was increased by >20-fold, compared to individual-exon RNAs (lanes 3 and 4). L binding to the three-exon RNA was stable at 200 mM salt, and reduced by only ~50% at 300 mM salt (lanes 4, 8 and 13). The dramatic increase in L binding to the exon 4-5-6 RNA suggests the formation of a salt-stable complex, containing both L and LL. In addition, a mutant derivative of exon 4-5-6 RNA (exon 4*-5-6*, containing the 4/5′CA and 6/m + 3′CA silencer mutations), showed strongly reduced affinity towards L/LL, and increased salt sensitivity (lanes 4/5, 8/9, 13/14). Since the silencer mutations inactivate the major LL targets of alternative splicing regulation, this suggests that stable L association is mediated through LL.

Finally, we also determined which exons contribute to the assembly of this stable L/LL complex on the *CD45* pre-mRNA, using—under stringent conditions—mutant derivatives, where either of the three variable exons was substituted by heterologous sequence (CD45/DUP-ex4, -ex5 and -ex6; Figure 5B, lanes 15–18; for alternative splicing of these mutant *CD45* pre-mRNAs, see Supplementary Figure S1). Whereas the exons 4 and 6 substitutions resulted in a moderate to strong reduction of L/LL binding, the complete substitution of exon 5 even increased the L/LL binding efficiency. We conclude that for the assembly of the stable three-exon complex, exon 6 (with two silencers) is more important than exon 4 (with one silencer), but that exon 5 sequence is not required.

CD45 exons 4–6 dependent *in vivo* interaction of hnRNP L and LL

Our *in vitro* binding data suggest the formation of a stable complex on the *CD45* pre-mRNA containing both L and LL. Therefore we tested whether both paralogs interact *in vivo* with each other in a *CD45*-dependent manner, using cotransfection of FLAG-LL and the *CD45* minigene with all three variable exons in HeLa cells (Figure 6A). HeLa cells provide an ideal model system for this, since the *CD45* minigene reproduces the normal

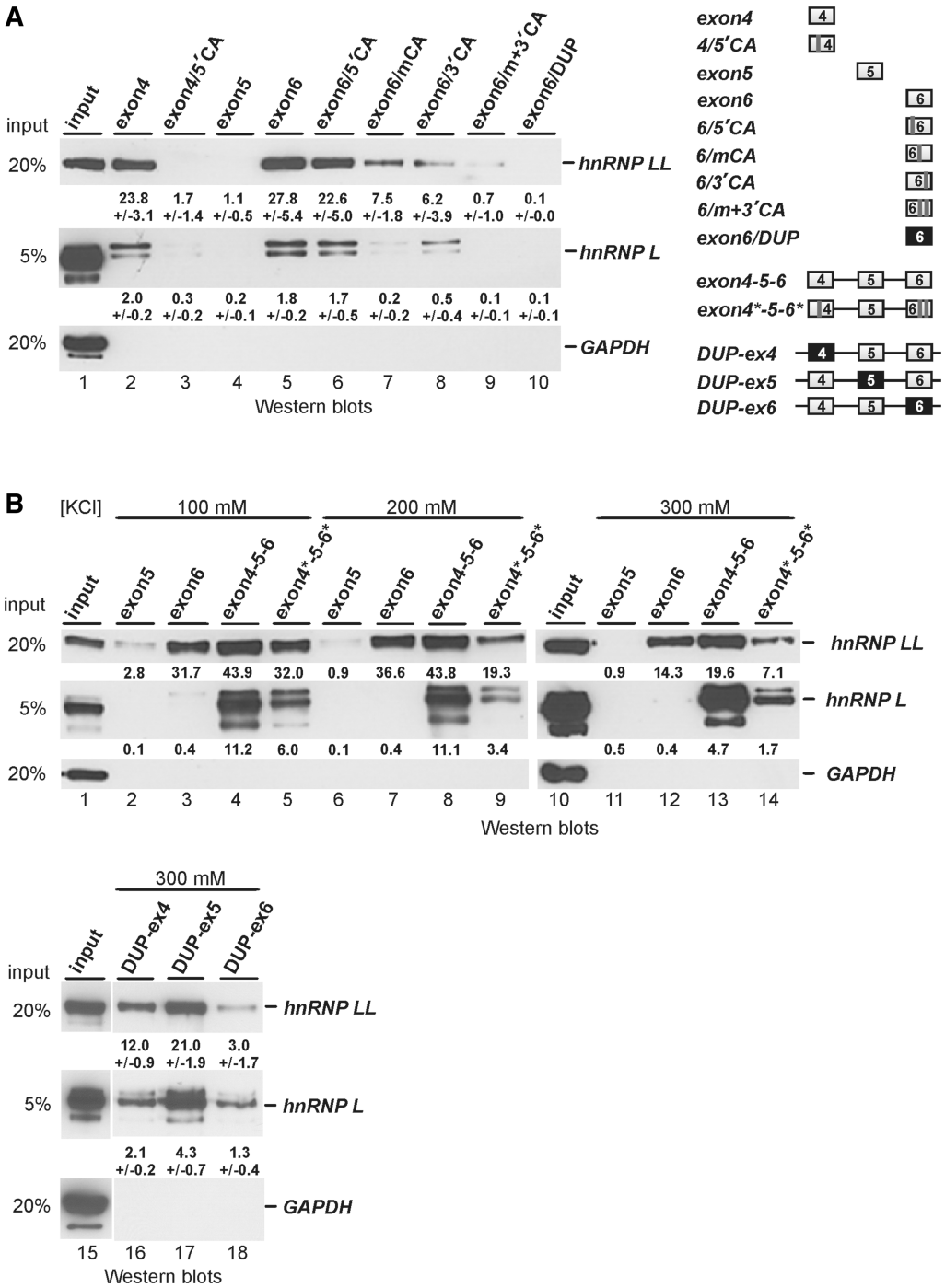

Figure 5. *In vitro* binding of hnRNP L and LL to *CD45* exons 4–6. (**A**) RNA binding of hnRNP L/LL correlates with repressor activity. Equimolar amounts of 3′-biotinylated RNAs, containing wild-type or mutant versions of each variable exon (as indicated above the lanes and schematically on the right), were prebound to Neutravidin agarose, followed by incubation in HeLa nuclear extract, washing at 100 mM KCl, release of bound protein and western-blot analysis for LL, L and, as a control, GAPDH. For comparison, nuclear extract input was analyzed in parallel (lanes 1; 20% for LL and GAPDH; 5% for L). Quantitation of L/LL pulldown is given below each lane (in % relative to the input, including SDs). (**B**) An RNA containing *CD45* exons 4-5-6 in *cis* stabilizes hnRNP L binding, depending on exons 4 and 6. As described in panel (A), pre-mRNAs, containing either the wild-type sequence (exons 4-5-6) or a mutant derivative, combining silencer mutations in exons 4 and 6 (exons 4*-5-6*), were compared with single-exons 5 and 6 RNAs for L versus LL binding in nuclear extract (lanes 1–14). Complex stability was tested by washing under different salt conditions (as indicated on top: 100–300 mM KCl). In addition, L/LL binding to mutant exon 4-5-6 derivatives were compared, in which one of the three exons was replaced by DUP sequence (DUP-ex4, -ex5 and -ex6; lanes 15–18).

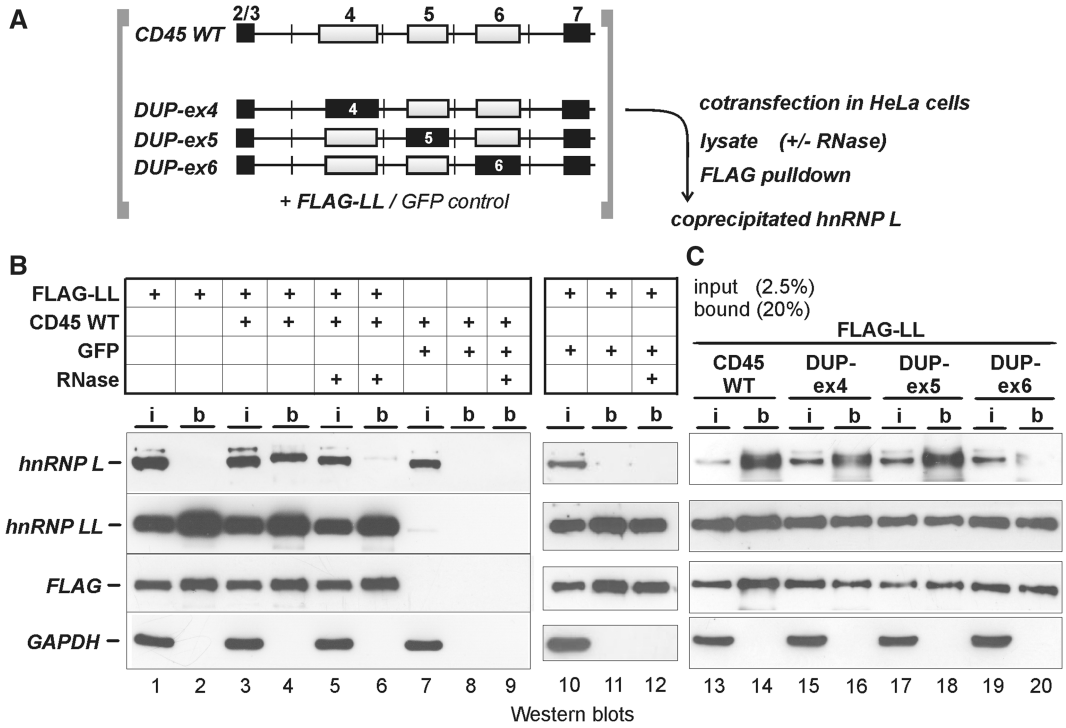

Figure 6. *CD45* RNA-dependent interaction of hnRNP L and LL *in vivo*. (**A**) Schematic of *CD45* minigenes and experimental protocol. (**B**) Interaction depends on CD45 RNA expression: HeLa cells were transfected with either FLAG-LL alone (lanes 1 and 2), or in combination with the CD45 WT minigene (lanes 3–6). As controls, CD45 WT was cotransfected with GFP (lanes 7–9), or FLAG-LL with GFP (lanes 10–12). Lysates were prepared without or with RNase treatment (as indicated), followed by FLAG pulldown assays. Coprecipitated L was detected by western blot, comparing input (lanes *i*; 2.5%) and bound material (lanes *b*; 20%), in parallel with LL, FLAG tag and loading control GAPDH. (**C**) Interaction depends on exons 4 and 6: Additional FLAG pulldown assays were performed after cotransfections of FLAG-LL and CD45 WT (lanes 13 and 14) or mutant minigenes carrying DUP-substituted exons 4–6 (DUP-ex4, -ex5, -ex6; lanes 15–20).

alternative splicing pattern (see above), and there is no endogenous *CD45* expression.

HeLa cells were transfected with the FLAG-LL expression construct, either alone or in combination with the *CD45* WT minigene. Lysates were prepared, treated with RNase or left untreated, followed by FLAG pulldown assays (Figure 6B, lanes 1–6) and western-blot detection of coprecipitated L (top panel), and, as controls, of transfected LL and GAPDH (middle and bottom panels). Comparing in each case input and FLAG-pulldown (bound; lanes *i* and *b*, respectively) clearly showed that L could be recovered only when *CD45* was cotransfected with LL (lanes 1–4). L coprecipitation depended on RNA (lanes 4 and 6), required FLAG-LL cotransfection (lanes 7–9), and was *CD45*-specific (lanes 10–12). L-LL interaction could also be detected in DG75 cells that express endogenous *CD45* (Supplementary Figure S2). Taken together, these data provide strong evidence for a stable, RNA-dependent and *CD45*-specific L/LL interaction.

Which of the three variable *CD45* exons is necessary for the L/LL interaction (Figure 6C)? In comparison to CD45 WT (lanes 13 and 14), we tested substitutions of either of the variable exons (DUP-ex4, -ex5 and -ex6; lanes 15–20). When exons 4 or 6 were substituted, L coprecipitation was consistently strongly reduced, in contrast to the exon 5 substitution. We conclude that exons 4 and 6 are particularly important for the *CD45*-dependent L/LL interaction.

DISCUSSION

B-cells as a new model system to study cooperation of the hnRNP L/LL paralogs in alternative splicing regulation

HnRNP L and LL are two paralogous RNA-binding proteins, closely related in domain organization, yet with different ranges of function and cellular distribution. Whereas the abundant L is clearly multifunctional, including its activity as a global splice regulator, LL appears to operate primarily in lymphocytes, with *CD45* pre-mRNA as its major target of alternative splicing regulation. Since both paralogs often coexist in the same cell type, this raises the question, whether and how they cooperate in splicing regulation. The same question applies to other known splicing regulators, that exist as paralogs, such as PTB/nPTB/ROD1 (33), Rbfox1/2 (34), ESRP1/2 (35), or the multiple members of the CELF and MBNL families (36).

Here we have introduced B-cells as a new model system to investigate the functional contributions of L versus LL in *CD45* alternative splicing regulation. In contrast to hnRNP L, LL protein expression strongly correlated with the terminally differentiated plasma cell state and with repression of the exons 4–6 unit (Figure 1). We selected one B-cell line, DG75, that does not express LL, providing a unique opportunity to study in a biologically relevant cell system the specific contribution of LL:

Clearly, LL overexpression was sufficient to switch *CD45* splicing from exon inclusion to the full-skipping form, consistent with CD45 isoform expression after LL overexpression and knockdown in BL41 or BJAB B-cell lines, respectively (19).

More insight into combinatorial *CD45* splicing was obtained by RNA-Seq analysis (Figure 2): Most striking was the effect of LL overexpression on skipping of all three variable exons, with exon 6 providing the major functional target of LL. Exon 5 repression was only detected in combination with exons 4 and 6, never by itself, that is no junction reads joining exons 4 and 6 were detectable. This is consistent with previous analyses of *CD45* alternative splicing in T-cells (37) and suggests that exon 5 is corepressed with its flanking exons 4 and 6.

Mutational analysis of CD45 combinatorial alternative splicing

We used a *CD45* minigene construct with all three variable exons 4–6, which allowed for the first time mutational analysis in their natural multi-exon context. Since the complex, L/LL-regulated *CD45* splicing pattern was reproduced in HeLa cells (Figure 3), this implies, first, that the minigene carries all essential regulatory sequence elements. Second, HeLa cells contain all necessary regulatory factors, and apparently, no additional lymphocyte-specific factors are required. The only difference between the splicing patterns of the *CD45* minigene in HeLa cells and the endogenous *CD45* in B-cells is the formation of the R45 form (HeLa cells) instead of the R56 form (B-cells). Most likely, this reflects the stronger repression of exon 6 by LL present in HeLa cells versus DG75 B-cells, where only L is present.

Individual knockdown of either L or LL in this system allowed monitoring the repressor activity of either paralog on each of the three variable exons (Figure 3): Clearly, exon 6 is specifically repressed by LL, not by L, whereas for exon 4 we detected strong repression by LL and a basal repressive function of L. In contrast, exon 5 by itself was not significantly repressed by either paralog. This indicates that exon 5 can be repressed only in combination with exons 4 and 6, consistent with our RNA-Seq data.

We used the *CD45* minigene to analyze potential silencer elements in their natural three-exon context (Figure 4). Silencer elements were predicted, based on our SELEX study (26) as clusters of three to four binding sites, separated by short spacers. In such a composite binding element three or all four RRMs of hnRNP L/LL would recognize individual adjacent motifs. We predicted a single silencer element in exon 4, and three in exon 6. For exon 5, no clustered binding motifs could be identified. In addition to alternative splicing, we also determined *in vitro* binding of L/LL to *CD45* variable exons 4–6, comparing the effects of these mutations (Figure 5).

The splicing analysis of the mutated *CD45* exons strongly supported the silencer elements predicted for exon 4 (4/5′CA mutant) and for two of the exon 6 elements (6/mCA and 6/3′CA mutants). Only the element predicted in the 5′ half of exon 6 (6/5′CA mutant) had no significant effects on alternative splicing nor binding, probably because it consists only of three motifs of the low-score type. Moreover, in all cases the effects on exon repression correlated very well with L/LL binding (compare Figures 4 and 5A). Since complete substitution of exon 4 (DUP-ex4) resulted in a nearly identical splicing pattern as the exon 4/5′CA silencer mutation, there appears to be only a single silencer in exon 4 (compare Figure 4A, lane 3, and Supplementary Figure S1A, lane 5). We conclude that this element in exon 4 and two silencer elements in exon 6 (mCA and 3′CA) mediate repression by L/LL.

How do these results compare with previous mutational data, all based on minigenes with single variable exons and studied in the T-cell system? Our predicted silencer element in exon 4 largely overlaps with the ARS element, which is necessary and sufficient for exon 4 skipping (38); in addition, Topp *et al.* (18) found that ARS mutation in exon 4 affects L/LL binding *in vitro*. Regarding exon 6, both strong silencers we identified based on predicted high-affinity L/LL binding sites (6/mCA and 6/3′CA) overlap with silencer-active regions mapped by linker-scanning mutagenesis (17).

Comparing the exon 6 mutations 6/mCA, 6/3′CA and the combination 6/mCA + 3′CA, we note that these resulted in similar effects, with increasing intensity. This strongly argues for two functionally independent silencers in the center and 3′ region of exon 6, which does not rule out the possibility that these two silencers may also partly synergize by increasing the local concentration of LL. With both of them inactivated, the R45 switches completely to the R56 form, which is paralleled by complete loss of L/LL binding to exon 6. We interpret this to reflect a competition between exons 4 and 6 for L/LL-mediated repression: In the WT situation, LL primarily targets exon 6 for repression, resulting in co-inclusion of exons 4 and 5 (R45 form); if after silencer mutation exon 6 cannot be repressed anymore, L/LL repress exon 4 with its lower-affinity silencer element better, thereby switching from exons 4–5 to exons 5–6 co-inclusion (R56 form).

Within exon 5 there are no predicted high-affinity binding sites for L/LL, consistent with lack of significant L/LL binding *in vitro*. Therefore we did not pursue detailed mutational analysis in this region; however, some conclusions can be drawn from substituting the entire exon 5 sequence (DUP-ex5). First, and in contrast to exons 4 and 6, substituting the exon 5 by heterologous sequence did not change the splicing pattern in the three-exon context, consistent with the idea that exon 5 is mainly co-regulated with its flanking exons 4 and 6 (Supplementary Figure S1A, lanes 2, 5, 8 and 11). Surprisingly, however, LL overexpression with the exon 5-substituted *CD45* did not shift all splicing to the R0 type, as in the case of the WT construct (compare lanes 4 and 10); this suggests that exon 5 corepression may require exon-specific sequences.

Model

In summary, we propose the following model to explain combinatorial alternative splicing of the three *CD45*

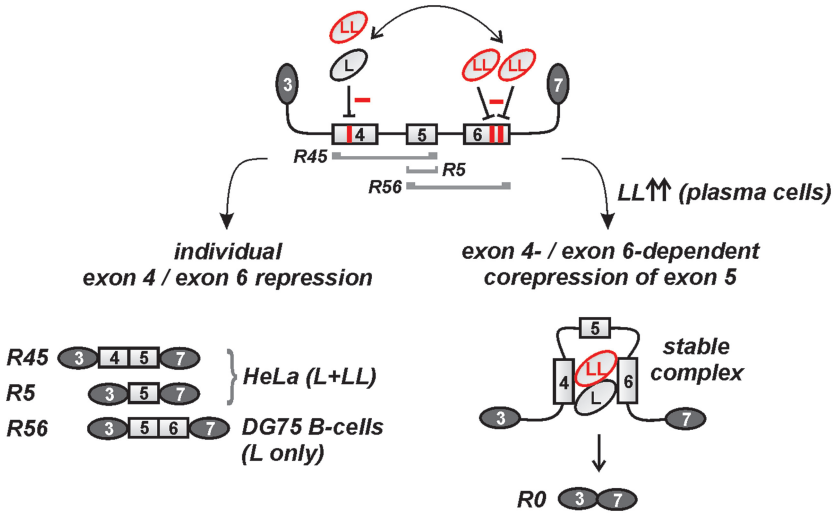

Figure 7. Model of *CD45* alternative splicing of variable exons 4/5/6, determined by combined activities of L/LL paralogs (for details, see 'Discussion' section).

variable exons (Figure 7). This model focuses on the cooperation of the paralogous L/LL factors, and does not take into account that additional factors may likely participate (39) and that cotranscriptional splicing (22) may add another level of regulation:

CD45 variable exons 4 and 6 are recognized by L and LL, requiring exonic splicing silencers in exons 4 and 6 (red bars). LL efficiently represses both exons 4 and 6, L preferentially exon 4. In contrast, exon 5 does not stably bind L/LL, and therefore cannot be repressed individually (no R46, but R45 and R56 forms). Instead, it is corepressed with exons 4 and 6. Which of the R45 or R56 form dominates, is determined by the presence of L versus LL (left part): If both L and LL are present (as in HeLa cells), exon 6 can be repressed individually, resulting in the R45 form, or both exons 4 and 6 are repressed, resulting in the R5 form. If only L is present (as in DG75 B-cells), exon 4 is repressed, resulting in the predominant R56 form. Additional supportive evidence comes from our mutational analysis: Successive weakening of the exon 6 silencers brings about a gradual shift from the R45 to the R56 form.

In addition to this individual exon 4 and exon 6 repression modes, our model proposes a repression mode depending on both exons 4 and 6 (right part). High LL levels (as in plasma cells) lead to a cross-exon 4–6 interaction and a stable RNP complex, in which exon 5 is looped out. This model is supported by both *in vitro* L/LL binding data and *in vivo* interaction assays: First, L binds to an exon 4-5-6 pre-mRNA with much higher efficiency than to the separate three exons, which can be explained by a stabilization or additional recruitment of L in the three-exon complex. Second, stable *in vivo* L-LL interaction depends on *CD45* RNA and on both exons 4 and 6, but not exon 5 sequence. As a result of the assembly of such a stable *CD45* pre-mRNA/L-LL RNP complex, with exon 5 looped out, all three variable exons are skipped, generating the R0 form.

SUPPLEMENTARY DATA

Supplementary Data are available at NAR Online: Supplementary Materials and Methods and Supplementary Figures 1 and 2.

ACKNOWLEDGEMENTS

We thank Florian Heyd and members of our group for discussions on the manuscript, David Ibberson, Bettina Haase and Dinko Pavlinic from the EMBL GeneCore sequencing team for excellent support and Heinrich Eckhof, Christian Preußer and Jingyi Hui for plasmid constructions. The results in this work are part of a dissertation (M.P.) submitted at the Justus Liebig University in Giessen.

FUNDING

Deutsche Forschungsgemeinschaft (grants DFG Bi 316/12, IRTG1384 and German-Israeli Project Cooperation Grant to A.B. and grants FOR832 and GK1660 to H.M.J.), IZKF Erlangen (to H.M.J.) and European-Commission-Funded Network of Excellence EURASNET (to A.B.). Funding for open access charge: Justus Liebig University of Giessen.

Conflict of interest statement. None declared.

REFERENCES

1. Wahl,M.C., Will,C.L. and Lührmann,R. (2009) The spliceosome: design principles of a dynamic RNP machine. *Cell*, **136**, 701–718.
2. Will,C.L. and Lührmann,R. (2011) Spliceosome structure and function. *Cold Spring Harb. Perspect. Biol.*, **3**, a003707.
3. Wang,E.T., Sandberg,R., Luo,S., Khrebtukova,I., Zhang,L., Mayr,C., Kingsmore,S.F., Schroth,G.P. and Burge,C.B. (2008) Alternative isoform regulation in human tissue transcriptomes. *Nature*, **456**, 470–476.

4. Pan,Q., Shai,O., Lee,L.J., Frey,B.J. and Blencowe,B.J. (2008) Deep surveying of alternative splicing complexity in the human transcriptome by high-throughput sequencing. *Nat. Genet.*, **40**, 1413–1415.
5. Cooper,T.A., Wan,L. and Dreyfuss,G. (2009) RNA and disease. *Cell*, **136**, 777–793.
6. Barash,Y., Calarco,J.A., Gao,W., Pan,Q., Wang,X., Shai,O., Blencowe,B.J. and Frey,B.J. (2010) Deciphering the splicing code. *Nature*, **465**, 53–59.
7. Thomas,M.L. (1989) The leukocyte common antigen family. *Annu. Rev. Immunol.*, **7**, 339–369.
8. Thomas,M.L., Reynolds,P.J., Chain,A., Ben-Neriah,Y. and Trowbridge,I.S. (1987) B-cell variant of mouse T200 (Ly-5): evidence for alternative mRNA splicing. *Proc. Natl Acad. Sci. USA*, **84**, 5360–5363.
9. Saga,Y., Tung,J.S., Shen,F.W. and Boyse,E.A. (1987) Alternative use of 5′ exons in the specification of Ly-5 isoforms distinguishing hematopoietic cell lineages. *Proc. Natl Acad. Sci. USA*, **84**, 5364–5368.
10. Streuli,M., Hall,L.R., Saga,Y., Schlossman,S.F. and Saito,H. (1987) Differential usage of three exons generates at least five different mRNAs encoding human leukocyte common antigens. *J. Exp. Med.*, **166**, 1548–1566.
11. Xu,Z. and Weiss,A. (2002) Negative regulation of CD45 by differential homodimerization of the alternatively spliced isoforms. *Nat. Immunol.*, **3**, 764–771.
12. Hermiston,M.L., Xu,Z. and Weiss,A. (2003) CD45: a critical regulator of signaling thresholds in immune cells. *Annu. Rev. Immunol.*, **21**, 107–137.
13. Hathcock,K.S., Hirano,H., Murakami,S. and Hodes,R.J. (1992) CD45 expression by B cells. Expression of different CD45 isoforms by subpopulations of activated B cells. *J. Immunol.*, **149**, 2286–2294.
14. Ogimoto,M., Katagiri,T., Hasegawa,K., Mizuno,K. and Yakura,H. (1993) Induction of CD45 isoform switch in murine B cells by antigen receptor stimulation and by phorbol myristate acetate and ionomycin. *Cell. Immunol.*, **151**, 97–109.
15. Lynch,K.W. and Weiss,A. (2000) A model system for activation-induced alternative splicing of CD45 pre-mRNA in T cells implicates protein kinase C and Ras. *Mol. Cell. Biol.*, **20**, 70–80.
16. Rothrock,C.R., House,A.E. and Lynch,K.W. (2005) HnRNP L represses exon splicing via a regulated exonic splicing silencer. *EMBO J.*, **24**, 2792–2802.
17. Tong,A., Nguyen,J. and Lynch,K.W. (2005) Differential expression of CD45 isoforms is controlled by the combined activity of basal and inducible splicing-regulatory elements in each of the variable exons. *J. Biol. Chem.*, **280**, 38297–38304.
18. Topp,J.D., Jackson,J., Melton,A.A. and Lynch,K.W. (2008) A cell-based screen for splicing regulators identifies hnRNP LL as a distinct signal-induced repressor of CD45 variable exon 4. *RNA*, **14**, 2038–2049.
19. Oberdoerffer,S., Moita,L.F., Neems,D., Freitas,R.P., Hacohen,N. and Rao,A. (2008) Regulation of CD45 alternative splicing by heterogeneous ribonucleoprotein, hnRNPLL. *Science*, **321**, 686–691.
20. Wu,Z., Jia,X., de la Cruz,L., Su,X.C., Marzolf,B., Troisch,P., Zak,D., Hamilton,A., Whittle,B., Yu,D. *et al.* (2008) Memory T cell RNA rearrangement programmed by heterogeneous nuclear ribonucleoprotein hnRNPLL. *Immunity*, **29**, 863–875.
21. Motta-Mena,L.B., Heyd,F. and Lynch,K.W. (2010) Context-dependent regulatory mechanism of the splicing factor hnRNP L. *Mol. Cell*, **37**, 223–234.
22. Shukla,S., Kavak,E., Gregory,M., Imashimizu,M., Shutinoski,B., Kashlev,M., Oberdoerffer,P., Sandberg,R. and Oberdoerffer,S. (2011) CTCF-promoted RNA polymerase II pausing links DNA methylation to splicing. *Nature*, **479**, 74–79.
23. Rossbach,O., Hung,L.H., Schreiner,S., Grishina,I., Heiner,M., Hui,J. and Bindereif,A. (2009) Auto- and cross-regulation of the hnRNP L proteins by alternative splicing. *Mol. Cell. Biol.*, **29**, 1442–1451.
24. Ray,P.S., Jia,J., Yao,P., Majumder,M., Hatzoglou,M. and Fox,P.L. (2009) A stress-responsive RNA switch regulates VEGFA expression. *Nature*, **457**, 915–919.
25. Hung,L.H., Heiner,M., Hui,J., Schreiner,S., Benes,V. and Bindereif,A. (2008) Diverse roles of hnRNP L in mammalian mRNA processing: a combined microarray and RNAi analysis. *RNA*, **14**, 284–296.
26. Hui,J., Hung,L.H., Heiner,M., Schreiner,S., Neumüller,N., Reither,G., Haas,S.A. and Bindereif,A. (2005) Intronic CA-repeat and CA-rich elements: a new class of regulators of mammalian alternative splicing. *EMBO J.*, **24**, 1988–1998.
27. Meister,S., Schubert,U., Neubert,K., Herrmann,K., Burger,R., Gramatzki,M., Hahn,S., Schreiber,S., Wilhelm,S., Herrmann,M. *et al.* (2007) Extensive immunoglobulin production sensitizes myeloma cells for proteasome inhibition. *Cancer Res.*, **67**, 1783–1792.
28. Brocke-Heidrich,K., Kretzschmar,A.K., Pfeifer,G., Henze,C., Löffler,D., Koczan,D., Thiesen,H.J., Burger,R., Gramatzki,M. and Horn,F. (2004) Interleukin-6-dependent gene expression profiles in multiple myeloma INA-6 cells reveal a Bcl-2 family-independent survival pathway closely associated with Stat3 activation. *Blood*, **103**, 242–251.
29. Rösel,T.D., Hung,L.H., Medenbach,J., Donde,K., Starke,S., Benes,V., Rätsch,G. and Bindereif,A. (2011) RNA-Seq analysis in mutant zebrafish reveals role of U1C protein in alternative splicing regulation. *EMBO J.*, **30**, 1965–1976.
30. Hui,J., Stangl,K., Lane,W.S. and Bindereif,A. (2003) HnRNP L stimulates splicing of the eNOS gene by binding to variable-length CA repeats. *Nat. Struct. Biol.*, **10**, 33–37.
31. Modafferi,E.F. and Black,D.L. (1997) A complex intronic splicing enhancer from the c-src pre-mRNA activates inclusion of a heterologous exon. *Mol. Cell. Biol.*, **17**, 6537–6545.
32. Willkomm,D.K. and Hartmann,R.K. (2005) 3′-Terminal attachment of fluorescent dyes and biotin. In: Hartmann,R.K., Bindereif,A., Schön,A. and Westhof,E. (eds), *Handbook of RNA biochemistry*. Wiley-VCH, New York, pp. 86–94.
33. Spellman,R., Llorian,M. and Smith,C.W. (2007) Crossregulation and functional redundancy between the splicing regulator PTB and its paralogs nPTB and ROD1. *Mol. Cell*, **27**, 420–434.
34. Zhang,C., Zhang,Z., Castle,J., Sun,S., Johnson,J., Krainer,A.R. and Zhang,M.Q. (2008) Defining the regulatory network of the tissue-specific splicing factors Fox-1 and Fox-2. *Genes Dev.*, **22**, 2550–2563.
35. Warzecha,C.C., Sato,T.K., Nabet,B., Hogenesch,J.B. and Carstens,R.P. (2009) ESRP1 and ESRP2 are epithelial cell-type-specific regulators of FGFR2 splicing. *Mol. Cell*, **33**, 591–601.
36. Kalsotra,A., Xiao,X., Ward,A.J., Castle,J.C., Johnson,J.M., Burge,C.B. and Cooper,T.A. (2008) A postnatal switch of CELF and MBNL proteins reprograms alternative splicing in the developing heart. *Proc. Natl Acad. Sci. USA*, **105**, 20333–20338.
37. Ratech,H., Denning,S. and Kaufman,R.E. (1997) An analysis of alternatively spliced CD45 mRNA transcripts during T cell maturation in humans. *Cell Immunol.*, **177**, 109–118.
38. Rothrock,C., Cannon,B., Hahm,B. and Lynch,K.W. (2003) A conserved signal-responsive sequence mediates activation-induced alternative splicing of CD45. *Mol. Cell*, **12**, 1317–1324.
39. Heyd,F. and Lynch,K.W. (2010) Phosphorylation-dependent regulation of PSF by GSK3 controls CD45 alternative splicing. *Mol. Cell*, **40**, 126–137.